

Heptadecane and Gallium Crystallization in Hydrodynamic Czochralski Model

Vladimir Berdnikov¹, Anatoly Prostromolotov^{2*}, Nataliya Verezub² and Victor Vinokurov¹

1. Institute of Thermophysics, Siberian Branch of Russian Academy of Sciences, Novosibirsk 630090, Russia

2. Institute for Problems in Mechanics, Russian Academy of Sciences, Moscow 119526, Russia

Abstract: The processes of convective heat transfer and crystallization were studied on basis of the simplified, but a unified calculation-experimental Czochralski model, using two materials with the melting temperature close to ambient room temperature: 1) heptadecane with a low thermal conductivity; 2) gallium with the high one. The transparency of heptadecane melt has permitted to visualize both the melt stream structures and geometry of its crystallized mass in the laboratory experiment and to provide data for verification of the corresponding calculation model. Numerical calculations have allowed to parametrically study the flow structure, heat fluxes on the cooled disk and to assess dependence of the melt-crystal interface for both these substances on the modes of convective heat exchange: thermal-gravitational and mixed (i.e., with an additional crystal rotation) convection.

Key words: Czochralski model, crystallization, fluid flows, heat transfer.

1. Introduction

Currently, mathematical modeling has become an important component in the development of technologies and equipment for crystal growth. The greatest progress has been achieved in the investigation of physical processes and in overcoming the computational difficulties in the course of modeling the convective heat and mass transfer for the Czochralski (Cz) crystal growth method. Contemporary conjugate mathematical models permit to determine thermal conditions and the impurity composition of the melt and crystal, change in shape of the MCI (Melt-crystal interface) and strain-stress state of the crystal.

They are calculated with provision for the complex radiation heat transfer, geometry and parameters of materials for the specific hot zones of Cz pullers. Similar models are implemented by means of modern software packages. However, adequate application thereof is hindered since they are cluttered up with

crude physical factors used in the models for specific processes and ambiguity of predetermined setting parameters for stability and accuracy of computation. Verification of the calculated results for such models is not sufficiently detailed.

The aim of this work was a detailed study of the processes of convective heat transfer and crystallization based on a simpler but unified calculation-experimental Cz crystallization model for the materials having T_M melting point close-to-ambient room temperature (heptadecane and gallium). This work presents a development of our surveys made without regard to the crystallization process, wherein ethanol was used as an operating medium [1].

The present computational model was developed on basis of AnsysFluent® code with added C++ UDF-subroutines written by authors. It has extended radically the ability of this code for specific tasks (for example, the rotation of crystallized fraction).

2. Physical Model

The laboratory unit is similar to the unit used in our

*Corresponding author: Anatoly Prostromolotov, Ph.D., professor, research fields: crystal growth, heat- and mass transfer, defects, simulations.

experiments with non-crystallizing medium – ethanol [1], its operating fragment is shown in Fig. 1. It comprises the following components: a cylindrical quartz crucible having an adiabatic bottom, a closed transparent heating chamber having double plexiglass walls, an upper foam plastic shield, removable disk mounted on the massive water-cooling shaft, a thermocouple probe and its moving mechanism, a high density foam plastic layers of thermal insulation.

Upset of the heat balance on a free surface is substantially excluded. For this purpose, the lateral surfaces of the shaft (4) and the disk (3) mounted thereon are thermally insulated by a foam layer in Fig. 1. The dense foam lid (8) insulates an air layer over a free surface from the ambient effects. An average temperature of the “crucible-melt-crystal” assembly is maintained as nearly as possible to ambient temperature. The absence of heat transfer from free surface has been provided by the absence of axial temperature gradient on this surface. For this purpose the temperature profile is controlled by special temperature measurements.

Fine aluminum particles (the flaky particles of the size ranging from about 10 to about 15 microns) were used to visualize the flow. All observations were made in the central cross-section by means of a planar light beam having a small thickness (1 - 2 mm). A digital video camera was used to measure the velocity field. The taken videos were enter into a computer and processed by the special software. Software processing permitted to plot the vector velocity fields and the instantaneous motion paths of traced melt.

The hot junctions of constantan-nichrome thermocouples of ~ 0.1 mm thick probe have been reduced to 10 - 15 microns for recording the melt temperature in the targeted points, including thin boundary layers. Special techniques were used for recording of statistical data (for $N = 2048$ time steps) with 0.2 - 0.5 s time interval between the measurements. 7 thermocouples were mounted on the crucible bottom and its sidewalls, 3 thermocouples – on

the disk for temperature monitoring in the radial and tangential directions. Average temperature drops between the crucible and the disk were to determine the Grashof numbers.

Contrary to Cz crystal growth, no crystal pulling occurs in this laboratory unit. However, created conditions for cooling of the shaft (4) maintain the set temperature $T_S < T_M$ on the bottom (3) of disk. Thus, in this instance, instead of the upward axial crystallization, the volume crystallization from a cold disk into the molten material is modeled. It is not a directional crystallization. The crucible is filled by molten materials, such as heptadecane or gallium, crystallizing at the ambient temperature. In the molten state heptadecane is transparent, but the transparency disappears in the course of solidification. The boundary of the melt and the crystalline fraction are distinctly visible and may be registered by a digital camera. Furthermore, the temperature may be measured by the thermocouple probe (9) in several reference points. Molten gallium is not transparent, therefore, only temperature was measured for it. The heat flux from the melt into the crystal, which has been registered for different convective modes, was of

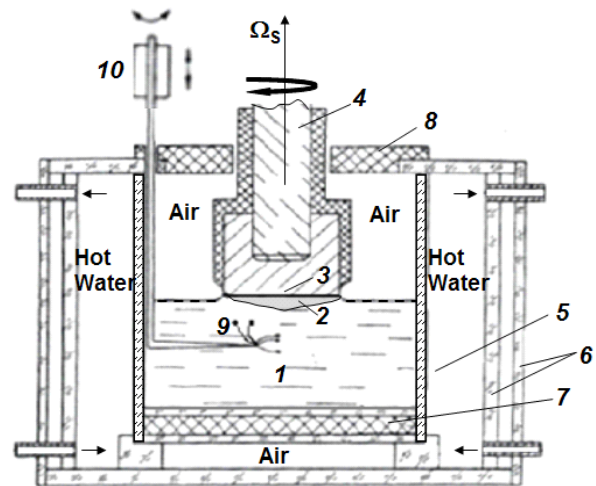


Fig. 1 The operating fragment of the physical model: molten mass (1) and crystalline portion (2) of the modeling material; bottom surface (3) of cylindrical water-cooled disk assembly (4); cylindrical crucible (5); heated chamber (6); layers of thermal insulation (7, 8); thermocouple probe (9) with displacement mechanism (10).

main interest. The operating zone geometry was as follows: $R_C = 0.1475$ m – radius of the cylindrical crucible, $R_S = 0.0536$ m – radius of the disk, H – variable height of the melt.

3. Mathematical Model

This mathematical model takes into account all above-mentioned specific features of the physical model. In this work the hydrodynamic approach of Cz crystal growth model has been used for calculations. In contrast to its previous versions [1], this model takes into consideration the crystallization process. The scheme of the model (Fig. 2) includes the cylindrical crucible ($R_C = 0.1475$ m, $H = 0.1032$ m; $H/R_C = 0.7$) filled by the melt, the coaxial disk ($R_S = 0.0536$ m; $R_C/R_S = 2.75$) which partially closes a free melt surface at the top. The model is supplemented by the temperature sensors (z, r) [m]: $S^1 - (0.0516, 0.0134)$; $S^2 - (0.005, 0.0134)$; $S^3 - (0.0516, 0.1425)$. As distinct from the previous modeling using Boussinesq approximation for ethanol flow, in this instance, given the crystallization process, the temperature variations of the following parameters are set: density $\rho(T)$, thermal conductivity $\lambda(T)$ and dynamic fluid viscosity $\mu(T)$.

It is assumed that an intermediate fraction (a crystallization region) is located between the crystalline (solid) and the molten (liquid) fractions at T temperatures, higher solidus temperature T_{SOL} and lower liquidus temperature T_{LIQ} , wherein linear variation of the molten portion is set by the following coefficient: $\beta = (T - T_{SOL}) / (T_{LIQ} - T_{SOL})$.

For a solid fraction and crystallization region the heat transfer equation at $T < T_{LIQ}$ is written with respect to enthalpy $h = C_p T$ as follows:

$$\partial(\rho h) / \partial t + V_p \partial(\rho h) / \partial z = \nabla(\lambda \nabla T) + Q,$$

where in C_p is heat capacity (constant value); V_p is constant rate of the crystal pulling along z axis; $Q = \rho H_L$ is a volume source taking into account of the latent heat H_L .

For a liquid fraction the heat transfer equation may be written as follows:

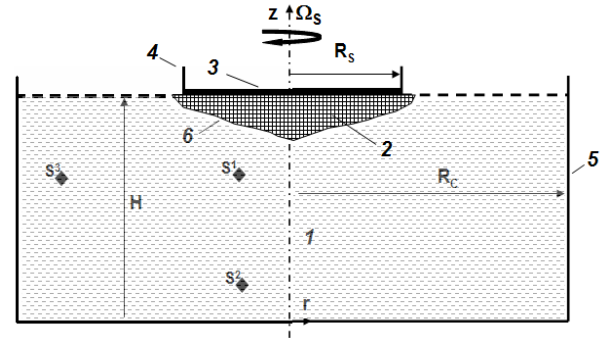


Fig. 2 The scheme of the mathematical model: molten (1) and crystalline (2) portions of modeling material; surface (3) of disk (4) thermostated at T_S ; cylindrical crucible (5) with the lateral wall thermostated at $T_W > T_S$ and thermally insulated bottom; MCI shape at melting point T_M (6); temperature sensors $S^1 - S^3$.

$$\partial(\rho h) / \partial t + \nabla(\mathbf{V} \rho h) = \nabla(\lambda \nabla T);$$

the equations of the melt motion and continuity are as follows:

$$\begin{aligned} \partial(\rho \mathbf{V}) / \partial t + \nabla(\rho \mathbf{V} \mathbf{V}) &= -\nabla p + \nabla(\mu \nabla \mathbf{V}) + \rho \mathbf{g}, \\ \text{div}(\rho h \mathbf{V}) &= 0, \end{aligned}$$

wherein \mathbf{V} is velocity vector, p is pressure, and \mathbf{g} is gravity vector.

According to this model, the crucible contains a molten fraction (1) of the material, which is crystallizing at melting point T_M . The molten state is ensured by heating the lateral wall (5) until temperature $T_W > T_M$.

The crucible bottom and the melt's free surface (dashed line) are adiabatic. The central part of melt surface is closed by a solid disk which is coaxial to the crucible. The temperature is supported at $T_S < T_M$ over the whole surface (3) of the cooled disk (4). This disk (4) may be rotated at rate Ω_S , and the melt is under gravity - \mathbf{g} .

Cooling of the disk results in crystallization of the molten material under the disk surface with formation of the solid region (2). Three sensors ($S^1 - S^3$) were placed in the melt for the recording the temperature filed changes. Then, these records were processed by the spectral analysis software.

In the course of these calculations the changes of MCI shape (6), depending on the convective modes at concrete temperatures (T_W, T_S) and on the rotation at

the rate Ω_S of the disk were studied. In this work we have studied the crystallization processes for the two materials crystallizing at the temperature close to ambient temperature (heptadecane: $T_M = 295$ K, gallium: $T_M = 302.8$ K).

The processes have been calculated for two modes of the convective heat transfer: 1) – in a separate action of thermal (thermo-gravitational and thermocapillary) convection, and 2) – in the joint action with a crystal rotation. It is noteworthy that an oxide film, formed on the open gallium surface in the ambient conditions suppresses the thermocapillary effect in the physical model without a vacuum chamber. Therefore, the thermocapillary effect is not taken into account in this calculation model. The thermal and physical parameters of used materials were taken from the reference books and are presented together with the values of the hydrodynamic similarity criteria in Table 1.

4. MCI Shapes in the Separate Action of Thermal Convection

The heating of the lateral crucible wall causes a thermal convection in the gravity field, wherein the heated melt moves upwardly along the wall to the cooled disk. This motion is enhanced by the action of thermocapillary forces on the free melt surface. The

solid fraction (2) (see Fig. 2) is crystallized near the disk. Its volume and shape dependent on the convective mode.

In above-mentioned mathematical model in the course of the experiment [2] the mode of thermal convection in molten heptadecane was considered at the following preset temperatures: $T_S = 292.53$ K – on the disk, and $T_W = 295.9$ K – on the lateral crucible wall. This mode was used for verification of results of the mathematical modeling.

Formation of the MCI shape was determined in accordance with the solidus contour T_{SOL} . The criteria values are provided in Table 1 for fixed temperature difference between the lateral wall and the disk $\Delta T = 3.37$ K. The performed calculations have shown an occurrence of a single-vortex steady flow (Fig. 3a). The velocity modulus reaches maximum value $V_m = 1.01 \times 10^{-2}$ m/s in the downflow near the axis. However, the buoyant flow near the lateral crucible wall occurs much more slowly ($V_m \approx 5.1 \times 10^{-4}$ m/s). The vertical stratification of the temperature field is formed, which is characterized both by the radial thermal homogeneity and by the fact that upper surficial molten layers are substantially more heated than its bottom layers. The essential temperature inhomogeneity arises under the crystalline region, wherein the cooled melt flows down along the MCI surface. In this instance contour T_{SOL} and experimental

Table 1 Thermophysical parameters.

Parameter	Heptadecane	Gallium
T_M – Melting point	295 K	302.8 K
ρ [kg/m ³] – Density	787 (273 K), 778 (295 K), 769 (303 K)	5904 (298 K), 6093 (303 K)
β_T [1/K] – Volumetric thermal expansion	1.17×10^{-3}	1.21×10^{-3}
ν [m ² /s] – Kinematic viscosity	5.187×10^{-6} (295 K)	3.24×10^{-7}
σ [N/m] – Surface tension	0.0281 (295 K), 0.0214 (373 K)	0.706 (323 K), 0.705 (373 K)
$\partial\sigma/\partial T$ [N/m \times K] – Surface thermal expansion	8.38×10^{-5}	2×10^{-5}
λ [J/s \times m \times K] – Thermal conductivity	0.1368 (295 K), 0.1319 (313 K)	28.1 (300 K), 26 (304 K)
C_p [J/kg \times K] – Heat capacity	2247	373
H_L [J/kg] – Heat of fusion	3.2×10^5	0.8×10^5
$Pr = \nu\rho C_p/\lambda$ – Prandtl number	66.37	0.026
$Gr = g\beta_T R_S^3 \Delta T/\nu^2$ – Grashof number	2.21×10^5	7.60×10^7
$Mn = (\partial\sigma/\partial T)R_S C_p \Delta T/\nu\lambda$ – Marangoni number	4.79×10^4	-
$Re = R_S^2 \Omega_S/\nu$ – Reynolds number	5.54×10^2	8.0×10^3

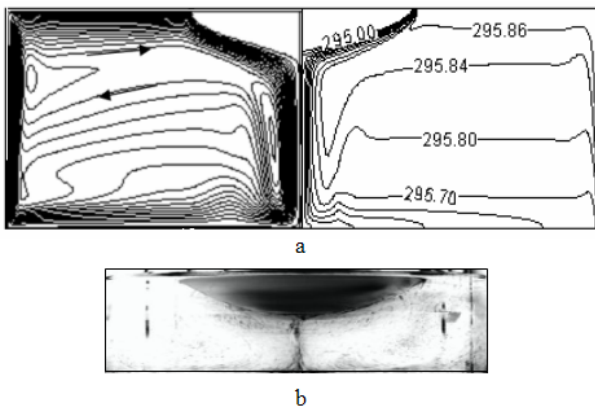


Fig. 3 Crystallization of heptadecane ($Pr = 66$) in the course of thermal convection ($T_S = 292.53$ K, $T_W = 295.9$ K, $Gr = 2.21 \times 10^5$): (a) streamlines (to the left of the axis) and temperature contours (to the right of the axis) with the MCI shape at $T_M = 295$ K; (b) photo of the crystalline portion of material (dark area).

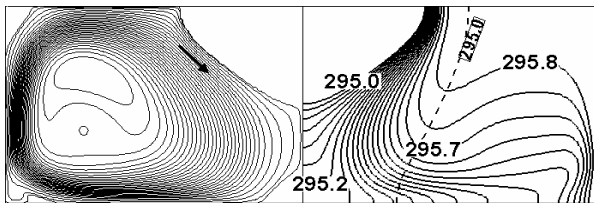


Fig. 4 Crystallization of the material with small Prandtl number ($Pr = 0.066$) in the course of thermal convection ($T_S = 292.53$ K, $T_W = 295.9$ K, $Gr = 3.8 \times 10^5$): streamlines (to the left of the axis) and temperature contours (to the right of the axis) with the MCI shape at $T_M = 295$ K.

photo of the MCI shape (Fig. 3b) agree satisfactorily with respect to the MCI convexity.

Investigation of possibilities of the MCI shape control is of special interest. For this purpose the MCI heptadecane shapes were calculated for different thermal convection modes depending: 1) – on Gr number and 2) – on variation of temperature difference ΔT . In the first instance, when preset temperature difference is $\Delta T = 3.37$ K, the convective modes were calculated for different Gr values from 22.1 till 2.21×10^5 . Their analysis showed that with the lowest Gr values, the stream velocity is small and heat transfer is performed in the thermal conductivity mode, and the solid phase encompasses the whole central region of the material. The Grashof number increase results in gradual decrease of vertical and

radial sizes of the crystalline portion.

The calculations provided for another temperature difference $\Delta T = 1.6$ K and $Gr = 1.1 \times 10^5$ complied with following preset temperatures: $T_W = 295.9$ K – on the lateral crucible wall and $T_S = 294.3$ K – on the disk. This convective mode differs from the modes mentioned above in slight temperature increase of the chilling disk that significantly affects the MCI shape straightening. Therefore, for the purposes of our objective, we can conclude that the MCI shape does not depend only on thermal convection intensity (or Gr number) and temperature difference between the heated lateral crucible wall T_W and crystallization temperature T_M , its shape also depends on the temperature T_S of cooling disk.

The regularities of the MCI shape alteration for the materials with a substantially higher thermal conductivity are also of interest. Such calculations were made for the modeling material having thermal conductivity 10^3 times higher than heptadecane. In this instance Prandtl number Pr for a molten portion was reduced to 0.066 and as a result corresponded to similar values of molten metals and semiconductors. The calculations were performed for approximately the same temperature parameters as for heptadecane: $\Delta T = 3.37$ K, $T_W = 295.9$ K, $T_S = 292.53$ K and within the same range of Gr number: from 380 till 3.8×10^5 . The MCI shape, streamlines and temperature contours for such modeling are shown in Fig. 4.

For a small Grashof number ($Gr = 380$) the crystalline portion occupies the whole crucible centre and corresponding MCI contour is shown by dashed line. In this instance, the flow is weak and heat transfer corresponds to the thermal conductivity mode. However, the stream becomes stronger with large Grashof number ($Gr = 3.8 \times 10^5$), which results in the substantial heating the crucible centre. It is obvious from the drawing of streamlines and temperature contours shown by solid lines. One may note some differences in the MCI shape compared to heptadecane.

For example, when Gr numbers are high, the

crystalline portion of this modeling material retains a solid phase shape, encompassing a greater volume of crucible centre. Thus it can be argued that dependence of the MCI shape upon thermal convection for substances with higher thermal conductivity (metals, semiconductors) is much lower than for organic and oxide substances with low thermal conductivity.

The quantity-related generalizations were made on the basis of the calculation results. The graphs of the most important characteristics were plotted depending on Gr number for different temperatures T_S of the cooled disk, as well as for large and small Prandtl numbers. In this model, a lateral crucible wall was regarded as the heating source and a cooling disk plays a part of the heat sink. The calculations were performed until a thermal balance achieved, when the integral heat flux on the lateral wall slightly (no more than 5%) differed from the integral heat flux on disk. These graphs are shown in Fig. 5 for the convexity Δ of MCI shape and the heat flux on disk is expressed by the relative integral value of Nusselt number Nu . Nu was calculated as the ratio of the integral heat flux for specific Gr to its value in a thermal conductivity mode [2].

It is noteworthy that convexity Δ of the MCI shape decreases along with the increase of Gr number. Its larger values correspond to smaller Pr number (see curves 1 and 3). For example, at $Gr = 10^4$ its values differ by 2.5 times: $\Delta = 0.035$ m for large $Pr = 66.37$, and $\Delta = 0.087$ m for small $Pr = 0.066$. As noted above, a temperature change of cooling disk T_S causes significant decrease of the MCI convexity. For $Gr = 10^5$ and bigger Pr number the values of MCI convexity differ by 5 times: $\Delta = 0.025$ m for $T_S = 292.53$ K, and $\Delta = 0.005$ m for $T_S = 294.3$ K (see for comparison the curve 1 and the mark 2).

The graphs in Fig. 5 also show variation of the relative magnitude in the integral heat sink on the disk (Nu number), as a result of normalizing the initial value of heat flux for a specific Gr number to similar value thereof for the conductivity mode.

It shall be pointed out that the heat sink increases along with the increase of Gr number. Moreover, this growth is much faster for larger Pr numbers (see for comparison the curves 1, 3, 4). For $Gr = 10^5$ these values differ by about 1.7 times ($Nu = 3.1$ for $Pr = 66.37$, and $Nu = 1.8$ for $Pr = 0.066$). According to [2] the data for the curve 4 were obtained at small Pr (0.05).

It is noteworthy that they well conform to the results of this work, when $Pr = 0.066$ (curve 3). Changes of temperature T_S on the cooling disk also results in certain distinctions, too. For example, for $Gr \approx 10^5$ and a large Pr number the Nu values differ by about 1.1 times: $Nu = 3.1$ for $T_S = 292.53$ K, and $Nu = 3.4$ for $T_S = 294.3$ K (see for comparison the curve 1 and the mark 2). Such increase of heat sink is explained by the influence of a slight T_S increase on 1.77 K, which is substantially less than reduction of the MCI convexity caused by it.

5. MCI Shapes in the Joint Action of Thermal Convection and Crystal Rotation

The influence of crystal rotation on the MCI shape has been discussed for a long time (since the publication of [3]). It is based on the idea of the laminar

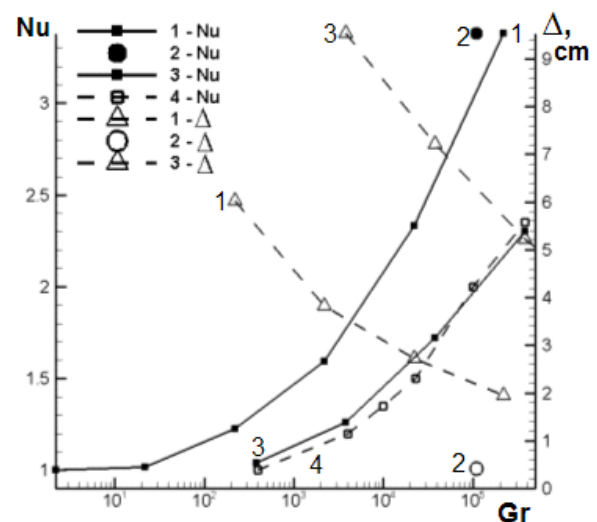


Fig. 5 Dependence of the MCI convexity Δ and Nusselt number Nu on Grashof number Gr with different Prandtl numbers Pr and temperatures of disk T_S : 1 – $Pr = 66.37$, $T_S = 292.53$ K; 2 – $Pr = 66.37$, $T_S = 294.23$ K; 3 – $Pr = 0.066$, $T_S = 294.3$ K; 4 – $Pr = 0.05$, $T_S = 294.3$ K.

= 292.53 K; $4 - Pr = 0.050$ [2].

two-vortex flow in the crucible. One vortex is caused by thermal convection in the heated crucible, and the other vortex, having the opposite motion direction, is caused by crystal rotation. In such arguments the MCI shape is not calculated, and its convexity or concavity is estimated qualitatively based on the ratio of Grashof and Reynolds numbers in the following way: $\gamma = Gr/Re^2$ or some other combination thereof. It is usually assumed that for $\gamma > 1$ thermal convection prevails, and the convex MCI shape emerges, while for $\gamma < 1$ – forced convection is caused by crystal rotation and provides the concave MCI shape. These views were helpful and were experimentally tested many times. In particular, the critical crystal radius corresponding to the MCI shape inversion (from strongly convex to slightly concave shape) was estimated for a stage of cone growth of a single crystal.

These ideas became the basis for a large number of works on numerical simulation of convective heat transfer in the hydrodynamic Cz model without due account for the crystallization process [4, 5]. Such works had practical importance because they took into consideration experimental studies. For example, in [5] the criterion for MCI shape has been selected on the basis of experimental observation of open molten surface in the course of a crystalline garnet growth.

Thus, the presence of petals on the open melt surface [6] corresponded to the concave (or flat) MCI shape and indicated prevalence of the forced convection caused by the crystal rotation. Otherwise, the thermal convection prevailed, and the MCI shape was convex. The means of efficient influence on the MCI shape proposed in [5] were based on the controlled changes of the crystal rotation rate during the growth process.

Currently, conjugated mathematical models taking into account the radiative heat exchange and crystallization are implemented actively into technological investigations. Different computational schemes are proposed on their basis. Their calculation results are used for improving the industrial Cz pullers

and crystal growth modes. However, until present the calculated results for crystallization process have not been verified in detail by physical modeling [7-9].

In this work such verification has been carried out on the basis of experimental data in respect of the heptadecane crystallization, characterized by large value of Prandtl number (similarly to oxide and organic materials): $Pr = 66.37$. Thermal conditions were set as follows: $T_S = 292.53$ K – on the disk and $T_W = 295.9$ K – on the lateral crucible wall (i.e. the temperature difference was $\Delta T = 3.37$ K). The combined actions of thermogravitational and thermocapillary convections were considered along with the forced convection caused by the disk rotation at angular velocity $\Omega_S = 1$ rad/s. The values of thermal parameters and calculated similarity criteria for this test are provided in Table 1.

In accordance with the flow pattern shown in Fig. 6a the main lifting motion is caused by thermogravitational convection near the lateral crucible wall. An average velocity of this lifting flow reaches 7.7×10^{-4} m/s. The flow is increased slightly by thermocapillary forces under the free molten surface in radial direction to the MCI. Cooling of the disk results in crystallization of a melt portion located under this disk with formation of a convex solidified region in the crucible. However, the disk rotation greatly influences on the melt flow under this solidified region.

Centrifugal forces during rotation of the solid convex region cause a vortex motion of forced convection, directed opposite to the vortex of thermal convection. The rotation velocity of the crystallized region reaches large value (5.56×10^{-2} m/s) and the whole molten volume is involved into rotating motion. However, intensity of the meridian flow (radial and axial velocity components) is significantly lower. Near the crucible's axis a molten material moves upwards with axial velocity $V_z \approx 4.14 \times 10^{-3}$ m/s and then it is thrown back in radial direction from the center by centrifugal forces, which has an effect on the solid convex surface.

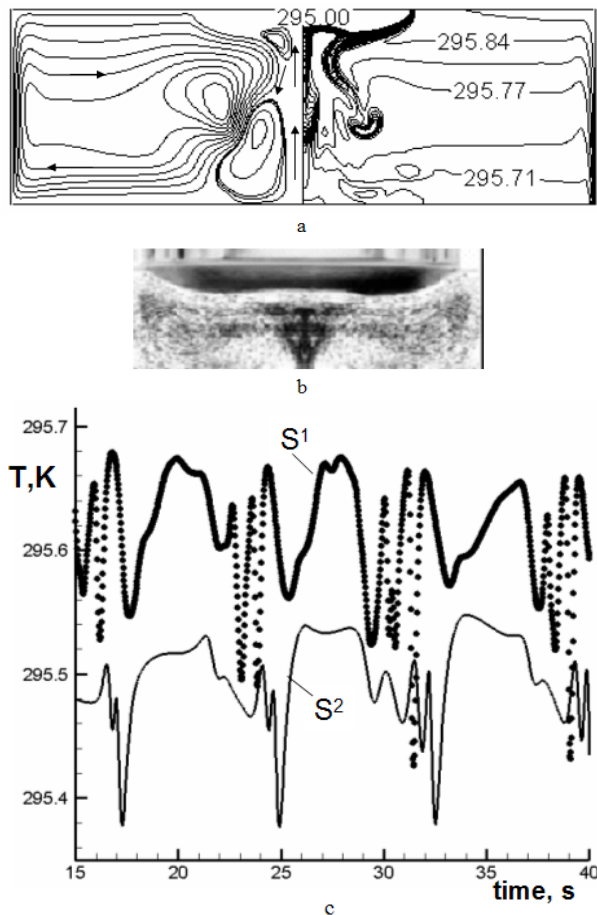


Fig. 6 Crystallization of heptadecane ($Pr = 66$) in the course of the joint action of thermal convection and crystal rotation ($\Omega_s = 1$ rad/s, $Re = 554$): (a) streamlines (to the left of axis) and temperature contours (to the right of the axis) with the MCI shape at $T_M = 295$ K; (b) photo of the crystalline portion of material (dark area); (c) graphs of temperature fluctuations in reference points S^1 и S^2 (see Fig. 2).

The counter-flow results in reduction of the impact of thermal convection on the MCI shape that creates its central upward bending, and such MCI shape is generally called a W-type. The calculated MCI shape presented by T_{SOL} contour and the experimental photo of the crystallized material agree well with each other (see for comparison Fig. 6b).

The estimations of the widely used parameter γ may be interested for practical purposes, too. In our case, its value was 0.72, which corresponds to the prevalence of forced convection ($\gamma < 1$), and it is consistent with the above-said results. It is noteworthy

that the above-said flow remains generally unchanged in time. However, the vortex intensity of the forced motion and thermal convection are oscillating depending on time. This oscillatory instability of two-vortex flow causes periodic occurrence, development and avulsion of “cold” plumes from the MCI (Fig. 6a). The “cold” plume phenomenon of heat transfer as applied to hydrodynamic Cz model (without for crystallization) was thoroughly considered earlier for a thermal convection in ethanol [1]. The present study shows the features of this phenomenon for heptadecane crystallization.

We assume that this fundamental phenomenon plays an important role in the formation of impurity striations in the course of crystal growth. This phenomenon is accompanied by substantial fluctuations of temperature and by variations of impurity concentration near the MCI.

It should be pointed out that the shape and location of MCI actually do not depend on time. However, a thermal boundary layer near the MCI is subject to the significant changes. The graphs of temperature fluctuations in 2 characteristic points of melt are shown in Fig. 6c. They show the significant temperature oscillations in point S^1 located near the MCI and its smaller oscillations in more remote point S^2 under the crystal. Moreover, the oscillations near the lateral crucible wall (point S^3) are actually absent. The most significant frequency of these oscillations corresponds to the range of 0.1-0.2 Hz for the point S^1 , which is consistent with set frequency of the disk rotation ~ 0.16 Hz. This indicates that a disk rotation rate significantly affects the “cold” plumes dynamics and frequency of temperature oscillations near the MCI.

The influence of crystal rotation rate has been thoroughly investigated for the gallium crystallization, which (as metals and semiconductors) has high thermal conductivity and, accordingly, small Prandtl number ($Pr = 0.026$). The melting point of gallium is higher ($T_M = 302.8$ K) than of heptadecane. Therefore, thermal conditions were different from the previous

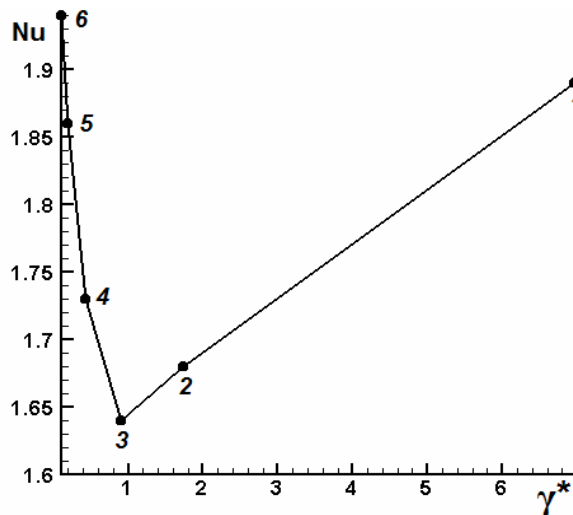


Fig. 7 Dependence of Nusselt number Nu on the hydrodynamic criterion γ^* . The calculated points conform to the following parameters: $Gr = 7.60 \times 10^7$, $Re \times 10^{-4} = 0.8 - (1), 1.6 - (2), 2.2 - (3), 3.2 - (4), 4.8 - (5), 6.4 - (6)$.

instance and were the following: $T_S = 299.43$ K – on the disk, $T_W = 303.8$ K – on the lateral crucible wall (i.e. the temperature difference was $\Delta T = 4.37$ K).

The rotation rate Ω_S of disk varied: 0.9, 1.8, 3.6, 5.4, 7.2 rad/s. Thermocapillary convection on the open molten surface was not taken into account. The Grashof number was constant: $Gr = 7.60 \times 10^7$, but the Reynolds number respectively varied: $Re \times 10^{-4}$: 0.8, 1.6, 2.2, 3.2, 4.8, 6.4. It was established that in the course of non-convective crystallization the crystalline region occupies a large central portion of the crucible. However, the joint action of thermal convection and crystal rotation results in its reduction and restriction by the convex MCI shape. This MCI shape slightly radially tapers, when $Re = 8 \times 10^3$ till 3.2×10^4 increases, and further increasing up to $Re = 6.4 \times 10^4$ also results in its axial compression.

Returning to the beginning of this section and to the discussion of the γ influence on the MCI shape, we can analyze dependence of Nu on different Re numbers for gallium crystallization. It is shown in Fig. 7 as a graph of integral Nusselt number on cooled disk: $Nu(\gamma^*)$, wherein γ^* parameter is defined as the multiplication of γ and $(H/R_C) \times (R_C/R_S)^2$. This is more reasonable and it means that in terms of

thermal convection a scale value takes into account melt depth H and a ratio of crucible radius R_C and crystal radius R_S . The Nu values were calculated on basis of the results of 6 variants submitted above. For all variants the Nusselt numbers provided in Fig. 7 were normalized to its value calculated in the thermal conductivity mode (without convection).

The plotted graph is non-monotonic, and its minimum corresponds to $\gamma^* \approx 1$, which can be the confirmation of correct selection of such criterion. With $\gamma^* > 1$ the vortex caused by thermal convection flows around the MCI shape, but with $\gamma^* < 1$ the vortex caused by the opposite director of the crystal rotation motion prevails in the crucible and it flows around the MCI shape.

6. Conclusions

This work has continued our studies of convective heat transfer in the course of Cz crystal growth on the basis of the unified physical and mathematical models. In our previous studies modeling was performed in the non-crystallizing medium (ethanol).

At this stage a convective heat transfer has been studied through using the materials (heptadecane and gallium), crystallizing at temperature close to the ambient room temperature. Contrary to modern conjugated mathematical models, which are overloaded by physical factors and adjusting parameters, indirectly supported by full-scale measurement, our simplified model uses reliable thermophysical parameters and data of physical modeling in strict adherence to the calculation parameters. The calculation model was developed on basis of the software AnsysFluent® code and our software routines, which have essentially expanded the basic possibilities of this package, in particular, for proper simulation of crystalline rotation.

An important advantage of physical modeling was thorough visualization of melt flow and crystallizing MCI shape in transparent melt of heptadecane. Its data have verified by the calculated results: the flow

structure, MCI shape and heat fluxes (Nu numbers) on the cooled disk and heated wall of crucible. This was done in 2 modes of heat transfer: 1 – only for thermal (thermogravitational and thermocapillary) convection and 2 – for mixed convection with due account for crystal rotation. For the first mode it was established that the MCI shape was affected by the intensity of thermal convection, depending on Gr number and determined by the temperature difference between heated crucible wall (T_w) and cooled disk (T_S).

The quantitative generalizations have been made on the basis of the calculations. The most important graphs (for the MCI convexity and Nu numbers) were plotted subject to Gr number and different temperatures of cooling disk T_S , as well as for large and small Pr numbers. It was established that the calculation results for rotating crystalline heptadecane complied with the relevant data of physical modeling. It was found out that vortex intensity affected by forced and thermal convections depended on time. Its oscillatory instability is manifested visually as a periodic occurrence, development and avulsion of "cold" plumes near the MCI. The graphs of temperature fluctuations and corresponding spectral density plotted for two characterizing points indicate that dynamics of "cold" plumes and corresponding frequency of temperature oscillations near the MCI substantially depend on the rotation rate of the disk.

The issues of influence of the crystal rotation rate on the MCI shape that have been discussed for years became clearer. In this respect, the influence of criterion $\gamma = Gr/Re^2$ on the gallium MCI shape has been analyzed. For this purpose the following modified parameter was used: $\gamma^* = \gamma \times (H/R_C) \times (R_C/R_S)^2$. Dependence of integral Nusselt number on this parameter on the cooling disk is non-monotonic, and it has its minimum at $\gamma^* \approx 1$. It is coherent with general conclusions of other authors that when $\gamma^* > 1$, the vortex caused by thermal convection flows around the MCI, while when $\gamma^* < 1$, the vortex of opposite direction caused by crystal rotation prevails in the

crucible and flows around the MCI.

Acknowledgments

This work was supported by the Russian Foundation for Basic Research (grants: 15-02-01794, 14-08-00454) and Siberian Branch of Russian Academy of Sciences (project III.18.2.5 State reg. 01201350443).

References

- [1] Berdnikov, V. S., Prostomolotov, A. I. and Verezub, N. A. 2014. "The Phenomenon of 'Cold Plume' Instability in Czocharlski Hydrodynamic Model: Physical and Numerical Simulation." *Journal of Crystal Growth* 401: 106-10.
- [2] Berdnikov, V. S., Vinokourov, V. A., Vinokourov, V. V., Gaponov, V. A. and Markov, V. A. 2011. "General Regularities of Convective Heat Transfer in the Crucible Melt-Crystal System of Czocharlski Method and Their Influence on the Solidification Front Shape." *Vestnik of the Lobachevsky State University of Nizhni Novgorod* 4 (3): 641-3.
- [3] Carruthers, J. R. 1976. "Flow Transitions and Interface Shapes in Czocharlski Growth of Oxide Crystals." *Journal of Crystal Growth* 36: 212-4.
- [4] Basu, B., Enger, S., Breuer, M. and Durst, F. 2001. "Effect of Crystal Rotation on the Three-Dimensional Mixed Convection in the Oxide Melt for Czocharlski Growth." *Journal of Crystal Growth* 230: 148-54.
- [5] Verezub, N. A., Nutsubidze, M. N. and Prostomolotov, A. I. 1995. "Convective Heat Transfer in the Melt during the Growth of Single Crystals of Garnet Structure by the Czocharlski Method." *Fluid Dynamics* 30 (4): 510-7.
- [6] Miller, D. C. and Pernell, T. L. 1982. "Fluid Flow Patterns in a Simulated Garnet Melt." *Journal of Crystal Growth* 58: 253-60.
- [7] Evstratov, I. Y., Kalaev, V. V., Zhmakin, A. I., Makarov, Y. N., Abramov, A. G. and Ivanov, N. G. et al. 2002. "Numerical Study of 3D Unsteady Melt Convection during Industrial-Scale CZ Si-Crystal Growth." *Journal of Crystal Growth* 237-239: 1757-61.
- [8] Vizman, D., Grabner, O. and Muller, G. 2001. "Three-Dimensional Numerical Simulation of Thermal Convection in an Industrial Czocharlski Melt: Comparison to Experimental Results." *Journal of Crystal Growth* 233: 687-98.
- [9] Muiznieks, A. and Krauze, A. 2006. "3D Transient LES Modeling of Turbulent Melt Flow in a Laboratory Model for Large CZ Industrial Silicon Crystal Growth Systems." In *Proceedings of the International Scientific Colloquium on Modelling for Material Processing (Riga, Latvia)*, 83-8.